VAS REGISTRATION ERRORS

UW/SSEC VAS PROGRAM
Paul Menzel

24 Feb 1976

Effects of Registration Errors on Clear Column Radiance Retrieval

Registration of fields of view (FOV) of different spectral bands using the same detector are subject to several errors. A number of these errors have been identified and their effect on sounding channel radiance retrievals has been studied by using retrieval algorithms with numerical simulation of radiance measurements. The results are presented in this report.

Registration errors that are considered in this work are tabulated below:

(A) Errors due to sampling line start timing.

(B) Errors due to equal angle (EA) resampling of S/C equal time (ET) samples.

(C) Subsatellite point motion (earth motion) due to orbit eccentricity and inclination to equatorial plane.

(D) Location errors due to nutation of satellite spin axis.

(E) Location errors due to motion of the scene.

Before discussing these registration errors, it is useful to briefly describe the technique used here for Clear Column Radiance Retrieval (CCRR). A more detailed discussion can be found in the SSEC final report on the SMS Sounder Specification. The technique utilizes the following fact: from a single FOV partially filled with clouds of a single type the radiance of one frequency is linearly related to the radiance of another frequency. Thus a plot of radiance measurements from a window channel I^W against I^S from a sounding channel for different effective cloud covers yields a straight line. By projecting two pairs of sounding and window measurements in different but geometrically adjacent FOV's, the clear column radiance of the sounding channel

can be obtained from the window channel clear column radiance. This Paired Field of View (PFOV) procedure is illustrated in Figure 1. It is important to note that the PFOV technique assumes that for a given pair the sounding and window channel radiances come from the same geometric FOV. If the sounding FOV is misregistered from the window FOV, then errors are introduced into the sounding clear column radiance retrieval (CCRR). Causes for such misregistration are now discussed.

The line start error in the SMS Line-Stretcher timing system has been investigated by L. A. Sromovsky (SSEC Annual Report, 1973). This error can be summarized from that report as follows: the jitter of the sun pulse output (peak value = .425 µsec) and the quantization of the Digital Phase Lock Loop (peak value = .1 µsec) combine for a line start timing error peak value of .53 µsec (1.4% of large detector FOV).

The present EA resampling system has two steps: first augment the ET samples with mid interval value determined by a four point interpolation, and then set the EA value to be that of the nearest ET value (actual or interpolated). A simulation of EA resampling of ET radiance measurements (real detector response of scene that has 100 ergs/etc jump) produced peak errors of 2.13 µsec (5.8% of large detector FOV).

Errors due to (A) and (B) occur randomly in each spin scan and can be reduced for any channel by multiple scanning. Ten scans would reduce the errors by a factor of $1/\sqrt{10}$.

Satellite orbital eccentricity and inclination with respect to the equatorial plane causes a twenty four hour periodic sub-satellite point motion that can be expected to be as large as 2° latitude (roughly 450 km north-south) and 1/2° longitude (roughly 50 km east-west). These periodic displacements correspond to a speed of roughly 60 km/hr for the path of the detector FOV

PFOV TECHNIQUE
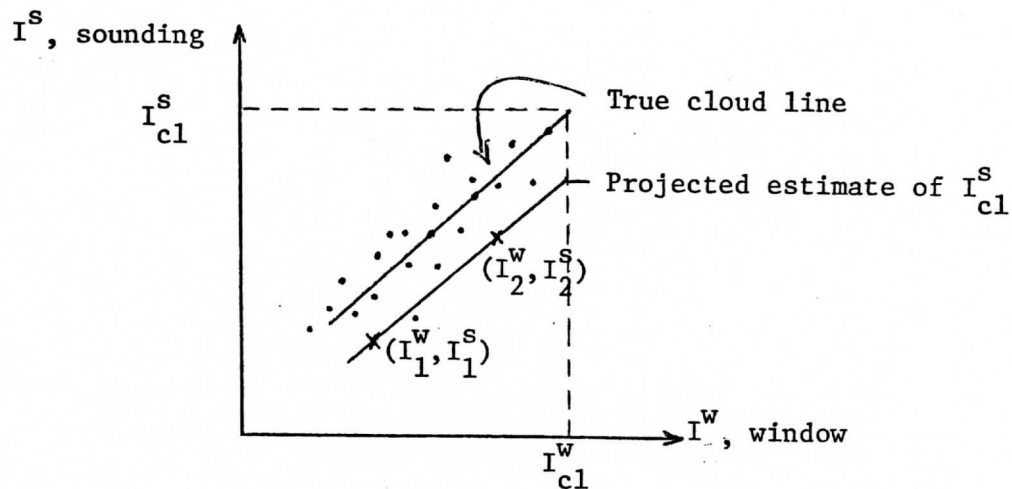
$$I^S_{cl} = \frac{I^S_1 - N^* I^S_2}{1 - N^*}$$

where

$$N^* = \frac{I^W_1 - I^W_{cl}}{I^W_2 - I^W_{cl}} = \text{ratio of cloud covers for two FOV's}$$

I^W_1, I^W_2 = window channel radiance measurements from two fields of view

I^S_1, I^S_2 = corresponding sounding channel radiance measurements.

I^W_{cl} = known window clear column radiance

I^S_{cl} = calculated sounding clear column radiance

FIGURE 1

on the earth surface. If there is a time interval of 30 seconds between the window channel and the more cloud sensitive sounding channels, then misalignments as large as .014 mrad (3.5% of a large detector FOV) are possible between the window channel and some sounding channels. For any given sounding channel this error depends on the order in which the bands are sampled; 30 sec is typical between window channel 8 and sounding channel 5.

Nutation of the S/C spin axis is caused in part by the scan mirror motion, SEM motion, and control jets. A passive damper reduces nutation amplitudes to .5 arc sec in times dependent on the magnitude of the induced nutation. The period of nutation is roughly 6 sec (less than 30 sec) so that maximum window and sounding channel misalignments due to nutation are .005 mrad (1.3% of large detector FOV).

Location errors are also caused by motions of the scene. A cloud at sub-satellite point with a speed of 30 km/hr can cause a maximum window to sounding channel misalignment of .007 mrad (1.8% of large detector FOV) in half a minute of sounding.

These errors (C), (D), and (E) can be reduced for a given sounding channel if the time between the window channel scan and sounding channel scans is reduced. Errors (C) and (E) could be halved if the time between window scans were halved. A summary of these peak registration errors is presented in Table 1.

If the sounding channel FOV is misaligned from the window channel FOV by as much as 5 or 10% of a FOV, how is the sounding CCRR affected? A numerical simulation procedure has been discussed in detail in several previous SSEC reports and will not be repeated here. The scenes used for the simulations are the Canary Islands and Mexico, both derived from Gemini

Table 1. Peak Registration Errors (given in % of large detector FOV = .384 mrad)

A. Line start timing   1.4

B. Equal angles (EA) resampling of
    equal time (ET) data   5.8

C.* Sub-satellite point motion
    (earth motion)   3.5

D. Satellite spin axis nutation   1.3

E.* Motion of clouds in scene
    (30 km/hr)   1.8

* Assuming 30 sec time interval between window and sounding channel observations.

photographs. The data grids representing these scenes contain an area
approximately 400 km square and have a resolution of 3.6 km (.1 mrad).
Measurements are simulated by weighting the radiances of the grid with an
ideal .4 x .4 mrad detector response function and sampling increments of
.1 mrad are implemented. Radiances are determined for channel 8 (window
channel) and channel 5 (sounding channel). Random correlated noise is added
to the radiances (noise equivalent radiance is .21 erg/etc for channel 8 and
.5 erg/etc for channel 5) and CCRR's are made using the Paired Field of View
(PFOV) technique. The results of ten noise additions are averaged and RMS
deviations are calculated to give statistical significance to the CCRR errors.
25% misalignment in the window channel with respect to the sounding channel
is acheived by shifting the grid over one .1 mrad column and reprocessing the
window channel radiances. Smaller misalignments are calculated from linear
combinations of the 0% and 25% misaligned radiances. Data is analyzed on
subgrids of 360 x 360 km, 90 x 90 km, 60 x 60 km, and 30 x 30 km. For each
subgrid a mean error and a weighted mean error is processed. The weighted

mean is calculated by weighting each pair retrieval radiance by the inverse of its variance. It should be remembered that errors must be less than .25 erg/etc if CCRR's are to be used for successful temperature soundings.

Results for the whole Canary Island Grid (CIG) are presented in Figure 2. As the misalignment increases a marked negative bias appears in the mean error. A major part of this bias is a consequence of the PFOV technique and is grid independent. For example, some negative bias occurs when the window channel sees a cloudless FOV and PFOV assumes the misaligned sounding channel FOV is also clear and then uses a cloudy FOV radiance for I_{cl}^{s}. The weighted mean error shows a reduction in error magnitude but still has the same trend toward negative bias with increasing misalignment.

Comparable mean error plots in Figure 3 for some of the 90 x 90 km subgrids (labelled from 1 to 16 as one reads across a page) show less uniformity from subgrid to subgrid, but nevertheless have similar overall behavior. The next figure shows similar information for all the subgrids. General behavior for small misalignments can be understood. When the window channel is misaligned into less cloudy regions, the mean error goes negative as a shift of the cloud line to the right would dictate (e.g. subgrid 13). Shifting the cloud line to the left, clear into cloudy, the mean error should go positive as subgrid 6 demonstrates.

Inspecting the data more closely reveals that for most subgrids a small number of pairs have CCRR's that are causing a large portion of the mean error. To prevent this a gated mean is evaluated using only pair retrievals within a standard deviation of the weighted mean. Selection of the best gate was done by maximizing subgrid data acceptibility while minimizing the rejection of pair retrievals within each subgrid. Figure 5 shows the

Distribution of the mean and weighted mean error
for different misalignments on the whole
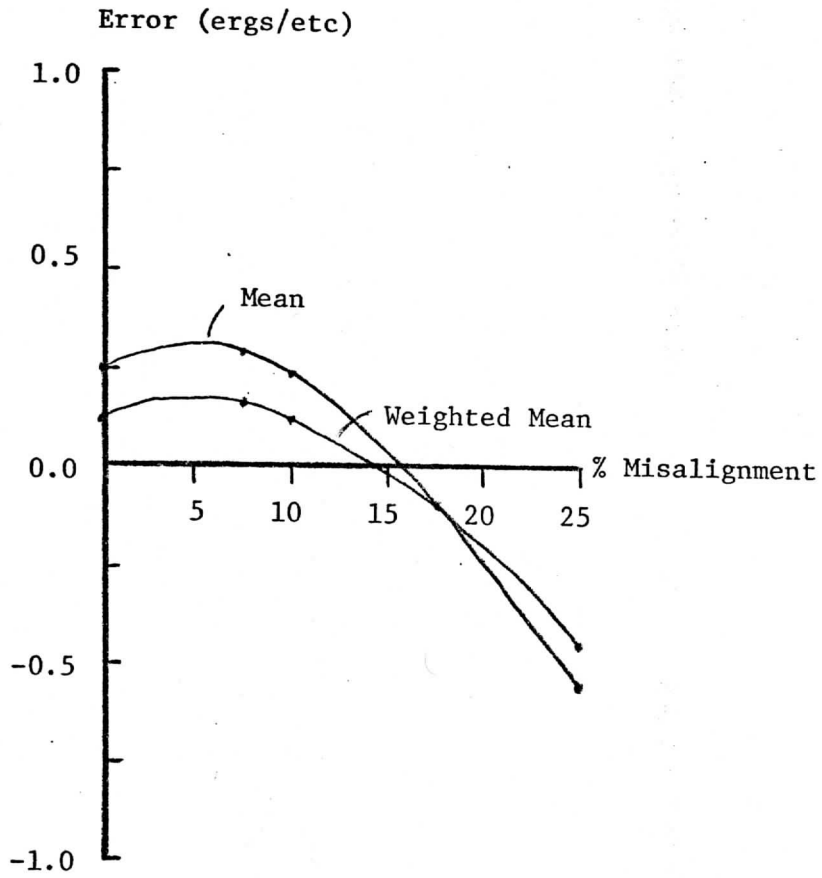Canary Island Grid

FIGURE 2

Distribution of the Mean Error for Different Misalignments
90 x 90 km Subgrids of Canary Island Grid
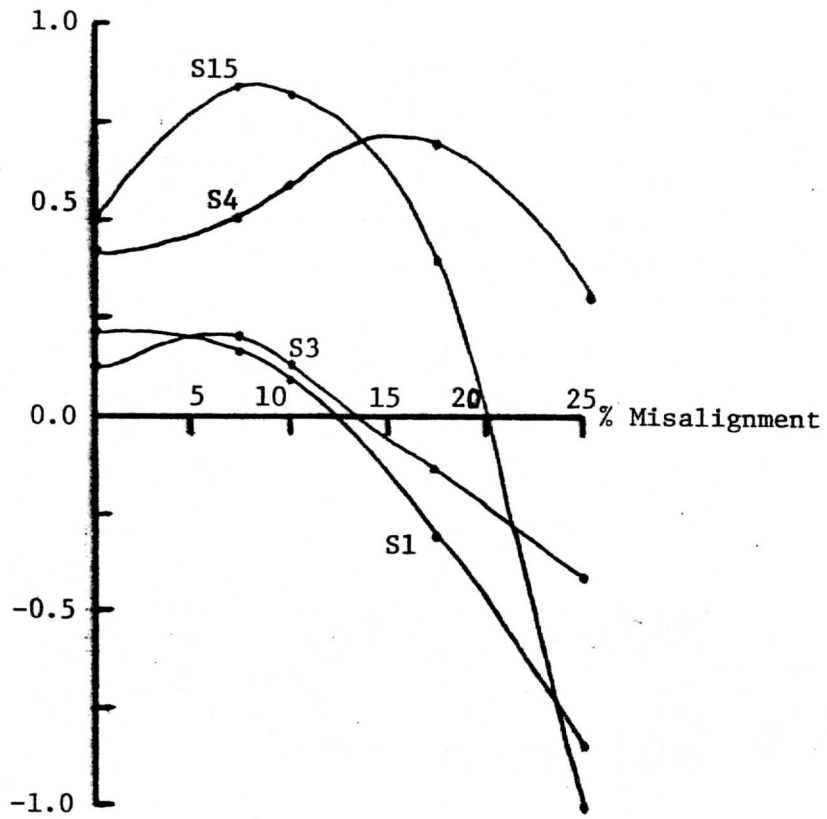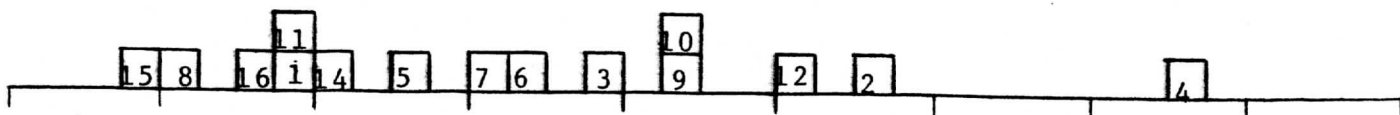
Mean Error (ergs/etc)

FIGURE 3

Distribution of the mean errors for different misalignments
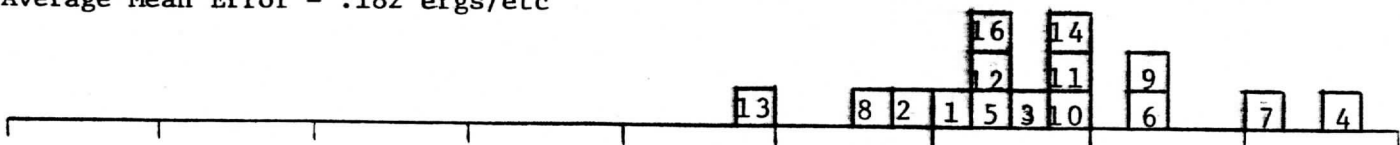90 x 90 km subgrids of Canary Island Grid

25% misalignment

Average Mean Error = -.617 ergs/etc

10% misalignment

Average Mean Error = .182 ergs/etc

No misalignment

Average Mean Error = .215 ergs/etc

Mean Error (ergs/etc)
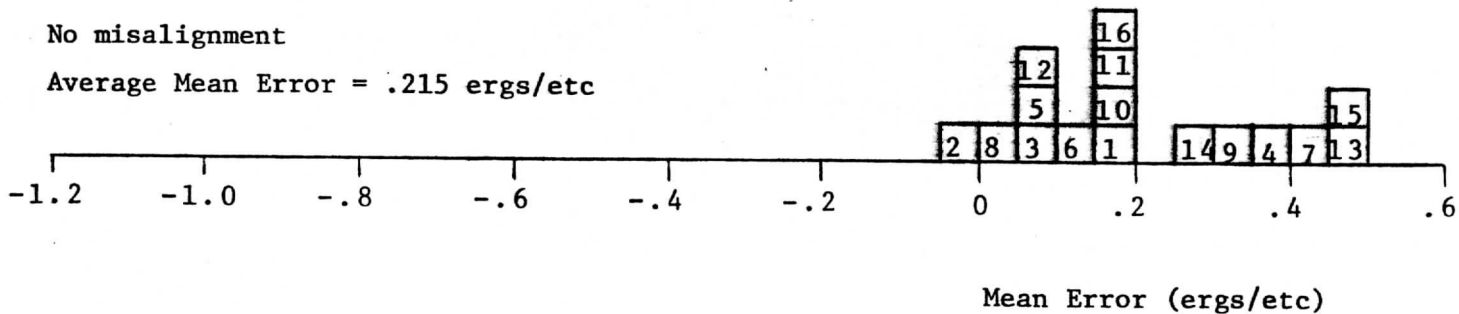
FIGURE 4

Mean errors with gates of different sizes for 25% misalignment
on 90 x 90 km subgrids of Canary Island Grid
No Noise
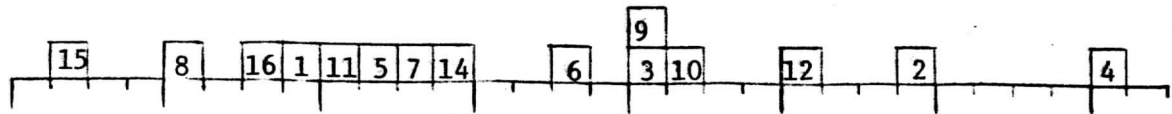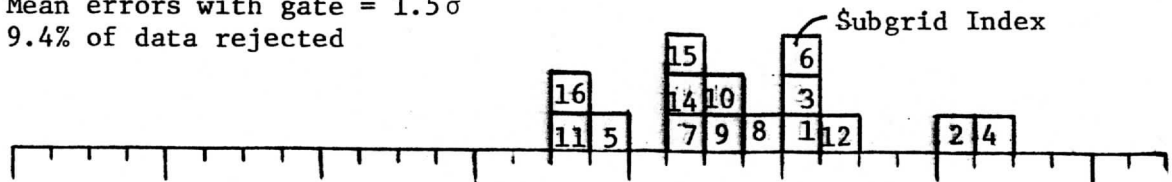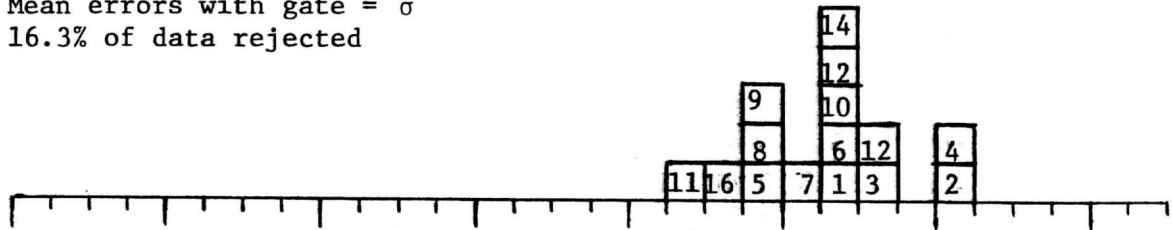
FIGURE 5

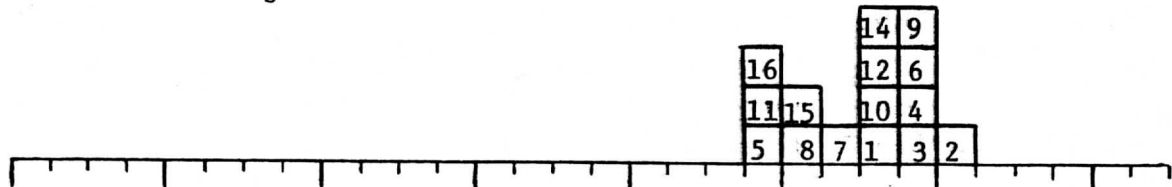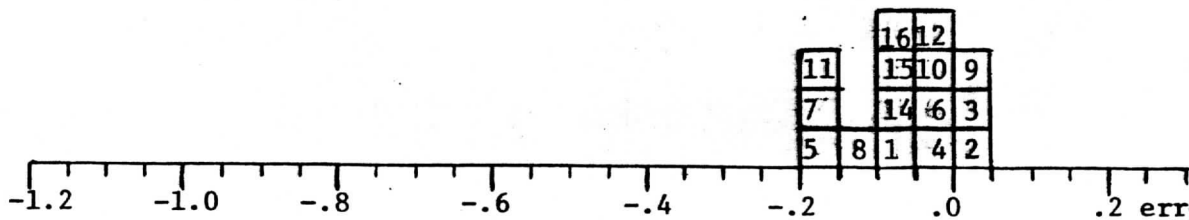effects of different size gates on subgrid radiances without noise. A gate of one standard deviation best satisfies our criteria. Figure 6 then shows the improvement achieved in the mean error by weighting and reaveraging with a gate; the average error for the 16 subgrids drops from .182 erg/etc to .061 erg/etc for 10% misalignment.

In Figure 7 plots of the weighted mean errors with a gate = σ show that for up to 10% misalignment 90 x 90 km resolution CCRR is very good, but that the results for 25% misalignment are unacceptable. It should be noted that the RMS of the ten noise runs is unaffected by misalignment and stays at .13 erg/etc. Also the loss of data as a consequence of using the gate only affected the RMS slightly, raising it up from .12 erg/etc to its indicated value.

A similar improvement in CCRR's for 60 x 60 km subgrids is shown in Figure 8. The weighting and gating of the means reduces the error from .223 erg/etc to .083 erg/etc at 10% misalignment. Clearly the data processing initiated for 90 x 90 km subgrids is just as effective for smaller resolutions. In Figure 9 we find that roughly 9 out of 10 subgrids are acceptable at up to 10% misalignment, but that only half are acceptable at 25% misalignment. The average noise RMS per subgrid is .20 erg/etc.

Finally at 30 x 30 km resolution (Figure 10) the weighted mean errors with a gate = σ show that one fourth of the subgrids are unacceptable with no misalignment, one third with 10% misalignment, and two thirds with 25% misalignment. The noise RMS per subgrid is .36 erg/etc, well above the tolerable level.

All the CIG radiance measurements cited in this paper so far were simulated with an ideal .4 x .4 mrad detector response (i.e. the detector output is proportional to the direct average of the scene radiance over the geometrical FOV of the detector). However, in reality, the detector

Distribution of errors at 10% misalignment for 90 x 90 km subgrids
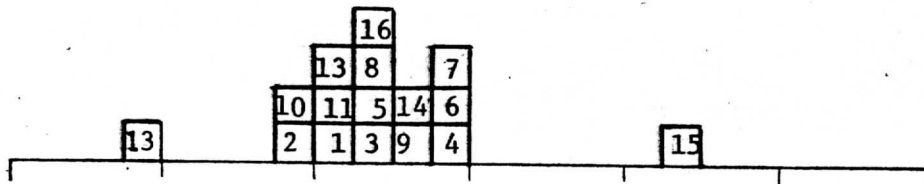of the Canary Island Grid; average of 10 noise runs

Mean errors, average = .182 ergs/etc.

Subgrid Index
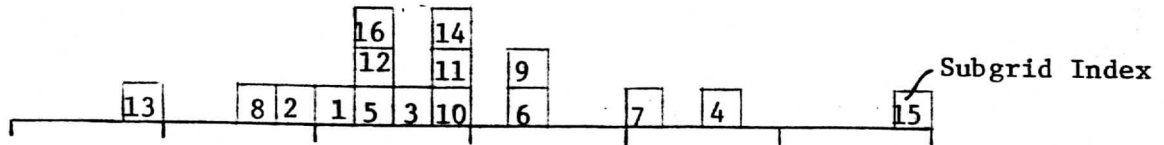
Weighted mean errors, average = .101 ergs/etc.
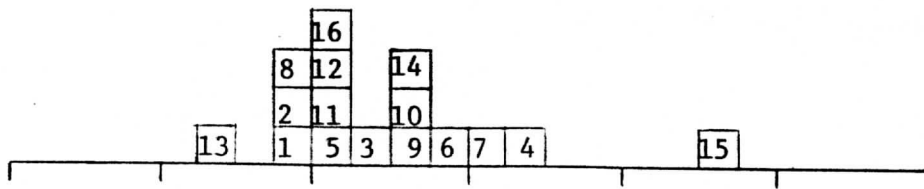
Mean errors with gate = σ, average = .085 ergs/etc.
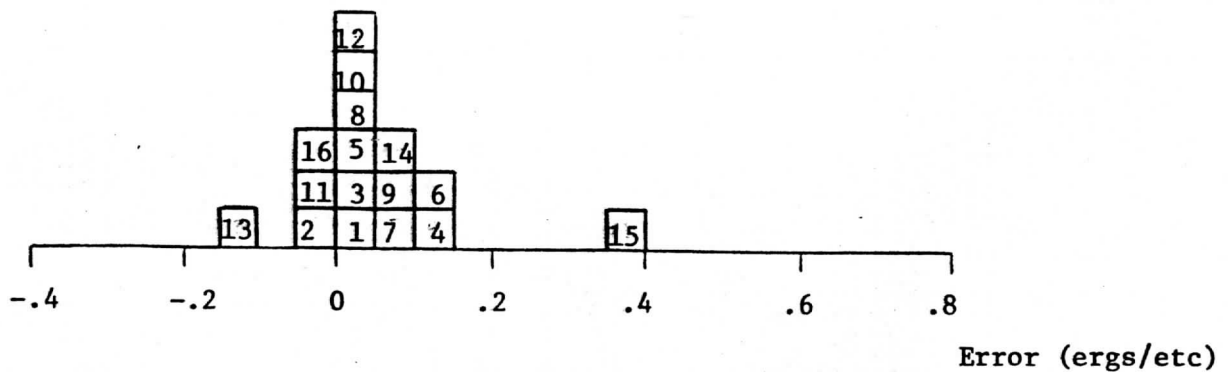
Weighted mean errors with gate = σ, average=.061 ergs/etc.

-.4   -.2   0   .2   .4   .6   .8

Error (ergs/etc)

FIGURE 6

Weighted mean error with gate = σ for different misalignments
on 90 x 90 km subgrids of the Canary Island Grid; average of
10 noise runs (average noise RMS per subgrid = .13 erg/etc).

FIGURE 7

Distribution of errors of 10% misalignment for 60 x 60 km subgrids
of the Canary Island Grid; average of 10 noise runs

Mean errors
average = .223 ergs/etc.

Weighted mean errors
average = .125 ergs/etc.

Mean errors with gate = σ
average = .113 ergs/etc.

Weighted mean errors with gate = σ
average = .083 ergs/etc.

-.4   -.2   0   .2   .4   .6   .8
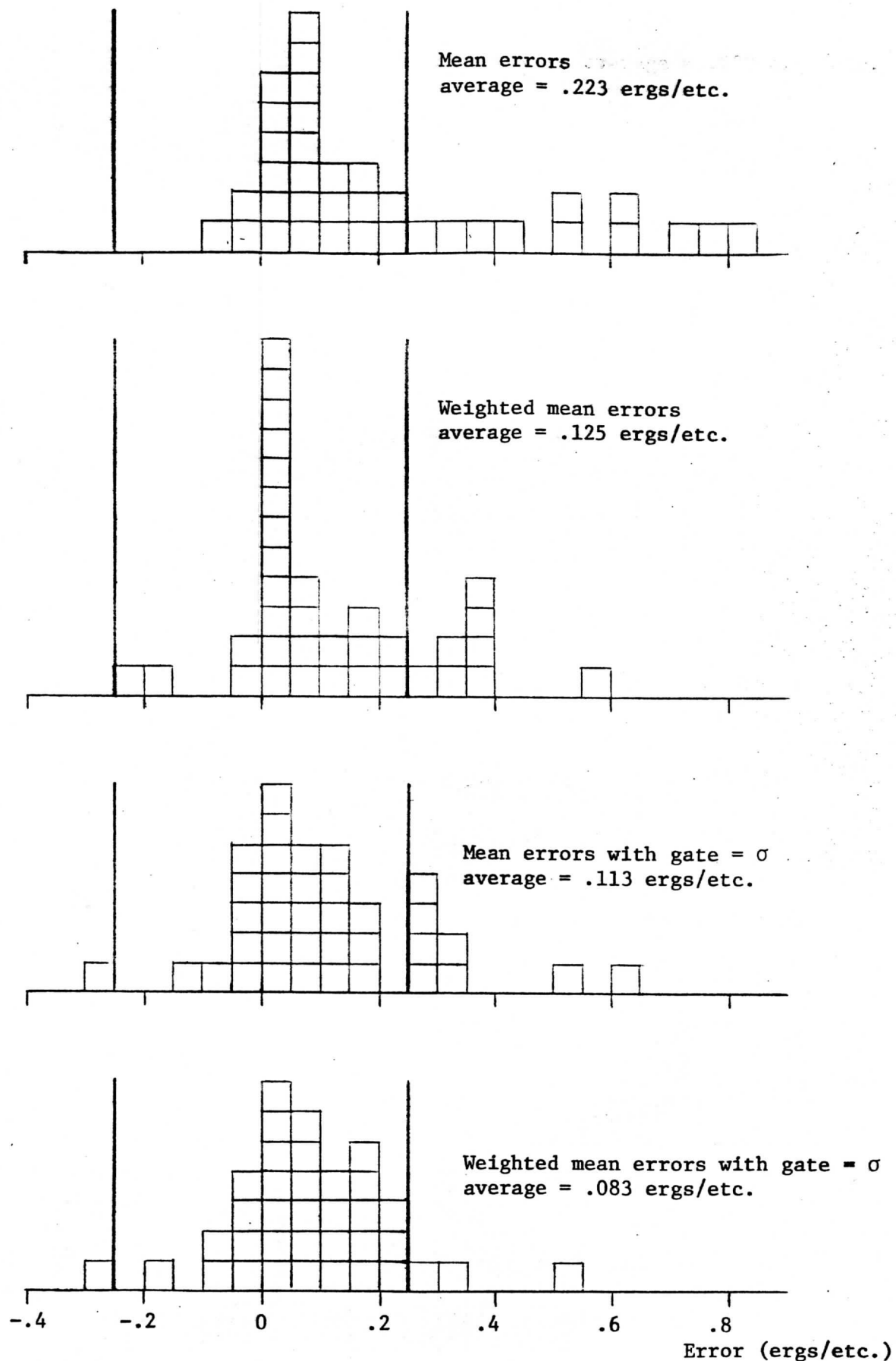
Error (ergs/etc.)

FIGURE 8

Weighted Mean Error with gate = σ for different misalignments
on 60 x 60 km subgrids of Canary Island Grid;
average of 10 noise runs
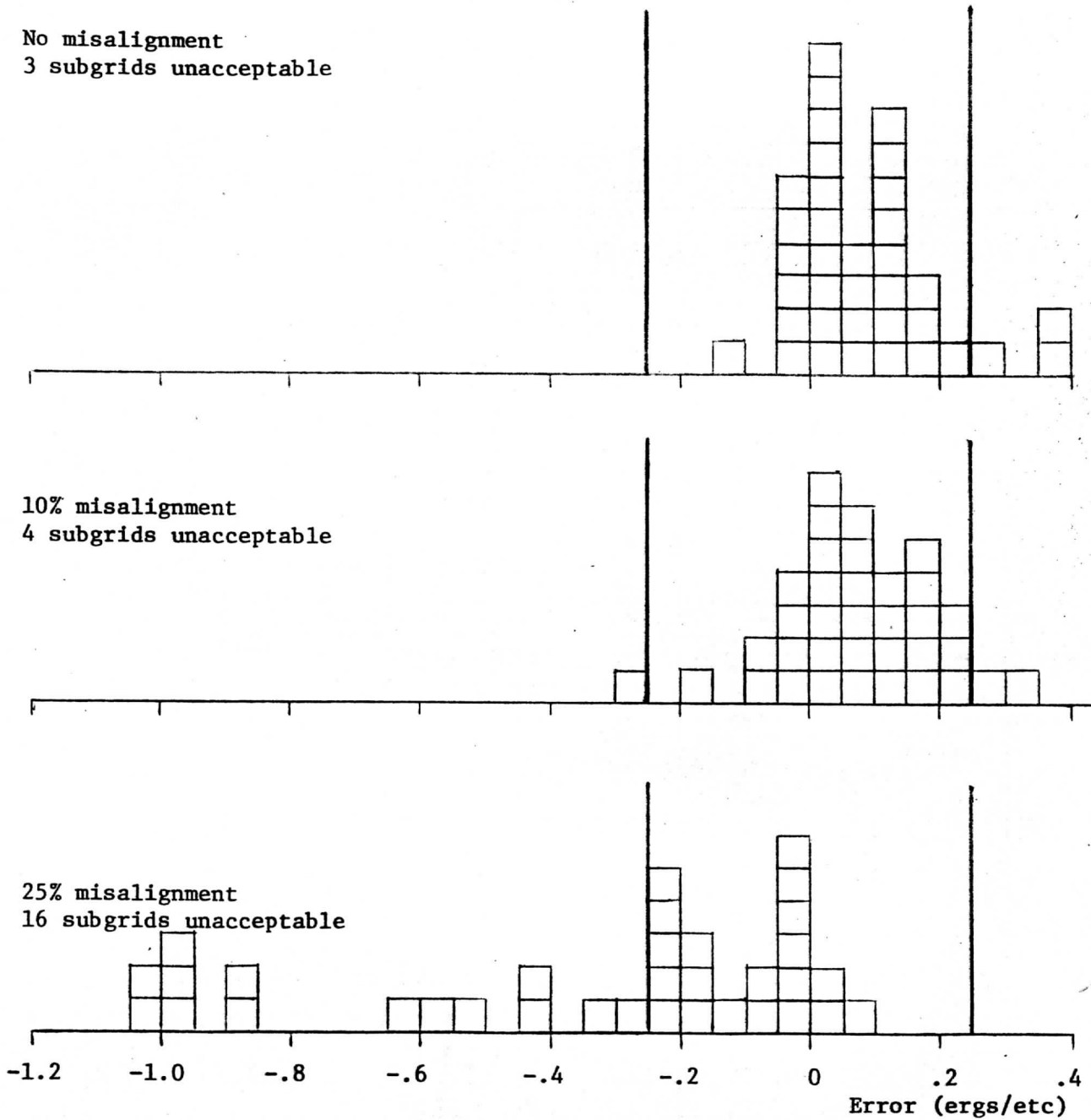(average noise RMS per subgrid = .20 ergs/etc).

No misalignment
3 subgrids unacceptable

10% misalignment
4 subgrids unacceptable

25% misalignment
16 subgrids unacceptable

-1.2   -1.0   -.8   -.6   -.4   -.2   0   .2   .4
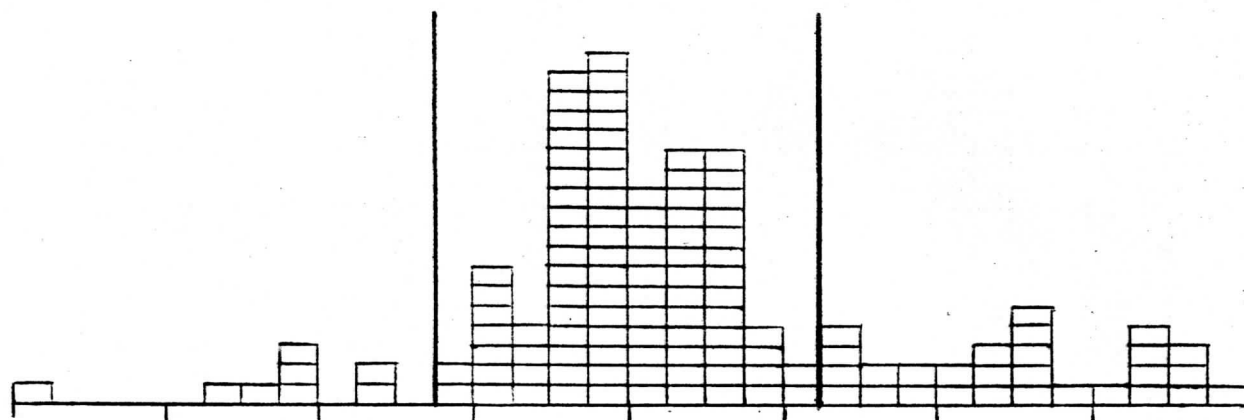
Error (ergs/etc)

FIGURE 9

Weighted mean error with gate = σ for different misalignments
on 30 x 30 km subgrids of the Canary Island Grid; average of
10 noise runs (average noise RMS per subgrid = .36 erg/etc).

No misalignment
38 of 144 subgrids unacceptable
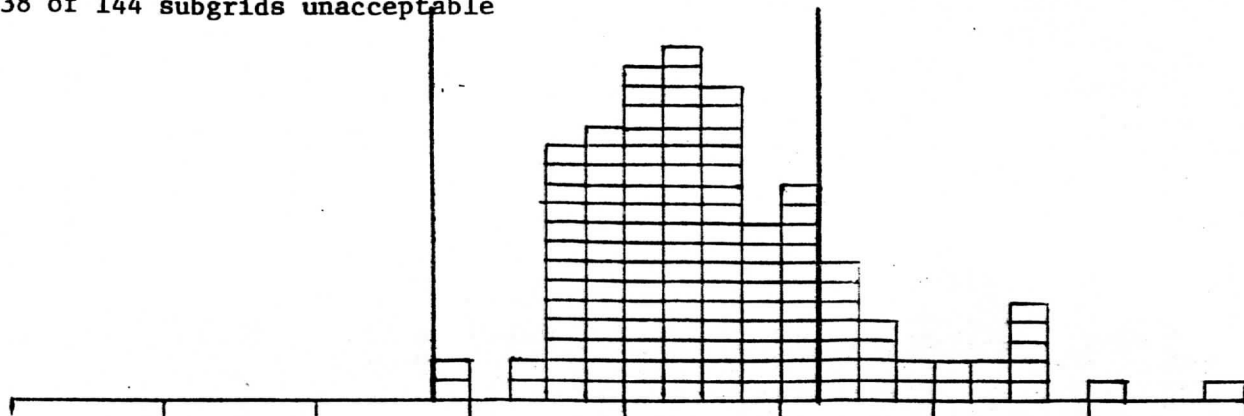
10% misalignment
52 of 144 subgrids unacceptable

25% misalignment
97 of 144 subgrids unacceptable

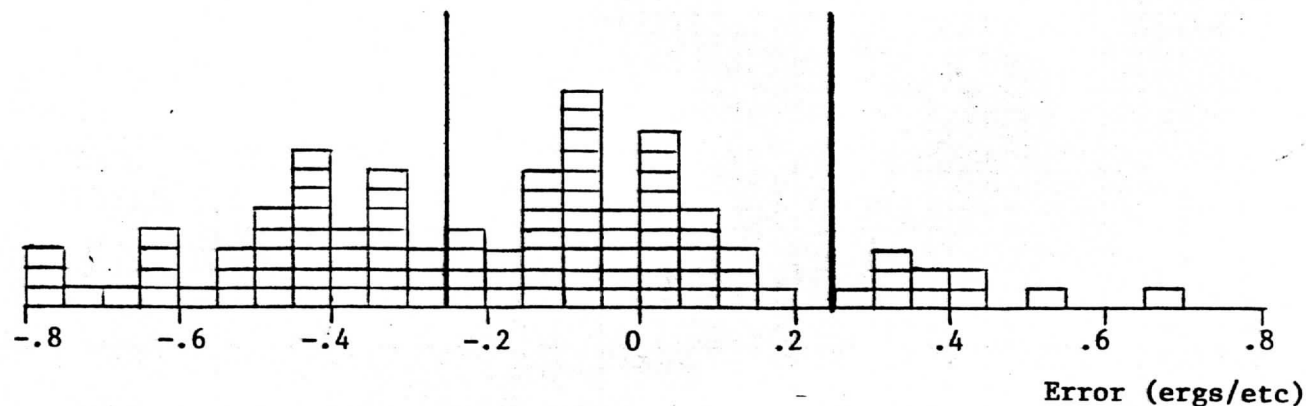-.8   -.6   -.4   -.2   0   .2   .4   .6   .8

Error (ergs/etc)

FIGURE 10

output is filtered so that each measurement is an unequally weighted time average of the field swept out by the detector FOV. In addition, diffraction effects reduce the detector response to scene radiances within the instantaneous geometric FOV and increase its response to those outside the instantaneous geometric FOV. Both effects can be simulated by a spatial weighting function which shall be referred to as the real detector response. Diffraction variations with wavelength will cause misregistration of different channels and hence effect sounding CCRR's.

To investigate the effect of diffractive misregistration on sounding CCRR's we reevaluate the mean errors shown in Figures 7, 9, and 10 and present the results in Figures 11, 12, and 13. The results are surprisingly similar. The diffraction misregistration causes a negative bias in the weighted gated mean for the whole grid of roughly .08 erg/etc at zero and 10% misalignment, but at 25% misalignment the effect is washed out. A noticeable shift to the negative is discernible at smaller misalignments for all three subgrid histograms, yet the percentage of subgrids yielding acceptable CCRR's is relatively unchanged. Thus diffractive misregistration does not pose any new problems.

All of the simulations shown have been performed with the Canary Island Grid. Similar tests have also been done with the Mexico Grid and the results are comparable. The same conclusions can be drawn from either grid and they are:

(1) For the current data acquisition scheme, peak misalignments of 5% to 10% of a large detector FOV can be expected.

(2) Earth motion and cloud motion misalignments (about 5% of FOV) can be reduced by shortening the time interval between sounding and window channels.

(3) EA resampling of ET data causes the largest misregistration (about 6% of FOV). Further study has indicated that utilization of a five point Lagrangian interpolation scheme reduces the peak misregistration to .24% of FOV. This however assumes exact knowledge of the location of the EA sample desired in relation to the available ET samples. Line start errors of .11 μsec RMS can be expected, hence the EA

location determination can be off by that amount. A five point Lagrangian interpolation scheme where the EA location is unknown to 2% of the ET sampling interval (somewhat larger than .11 μsec divided by ET sampling time of 8 μsec) produces peak misregistrations of .59% of FOV. This is a marked improvement over the present scheme and merits further attention.

(4) A gate of one standard deviation for reaveraging pair retrievals of the subgrid halves the mean error. A weighted mean error with gate = σ is roughly a third of the mean error.

(5) The .25 erg/etc requirement on CCRR accuracy is achievable for resolutions as small as 60 x 60 km and misalignments as large as 10%. Sounding at resolutions of 30 x 30 km will require reduced noise RMS and selection of relatively cloud free areas.

(6) Detection of cloud types by time sequence window channel scenes may help reduce the occurence of mixed cloud type pair projections, hence reduce errors. Preliminary investigations show that if the Canary Island grid is assumed to contain only one cloud type, then mean errors in PFOV retrievals are reduced by a factor of four for misalignments of 10% or less.

Weighted Mean Error with Gate = σ for different misalignments on
30 x 30 km CIG subgrids viewed with real detector response; average
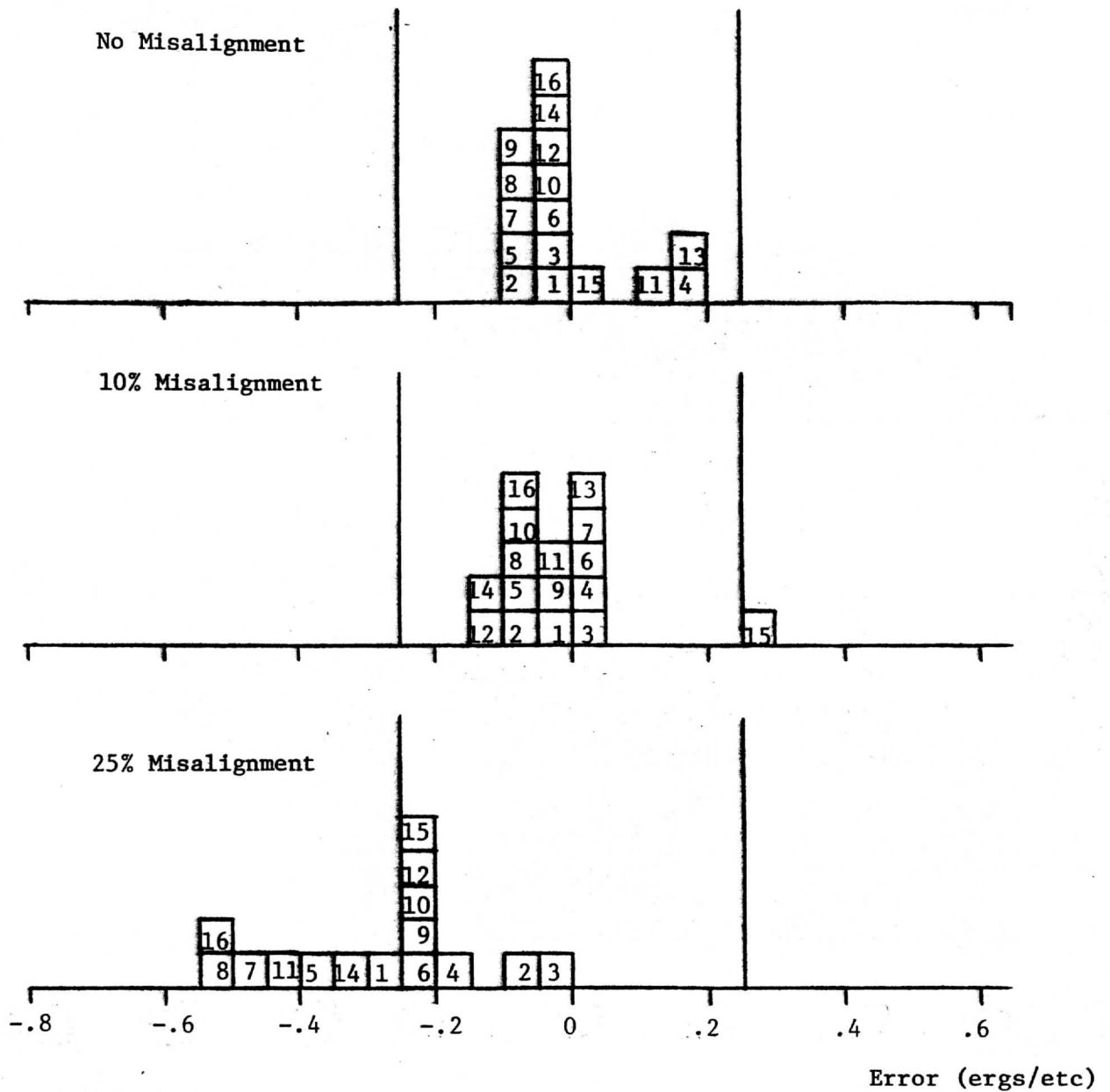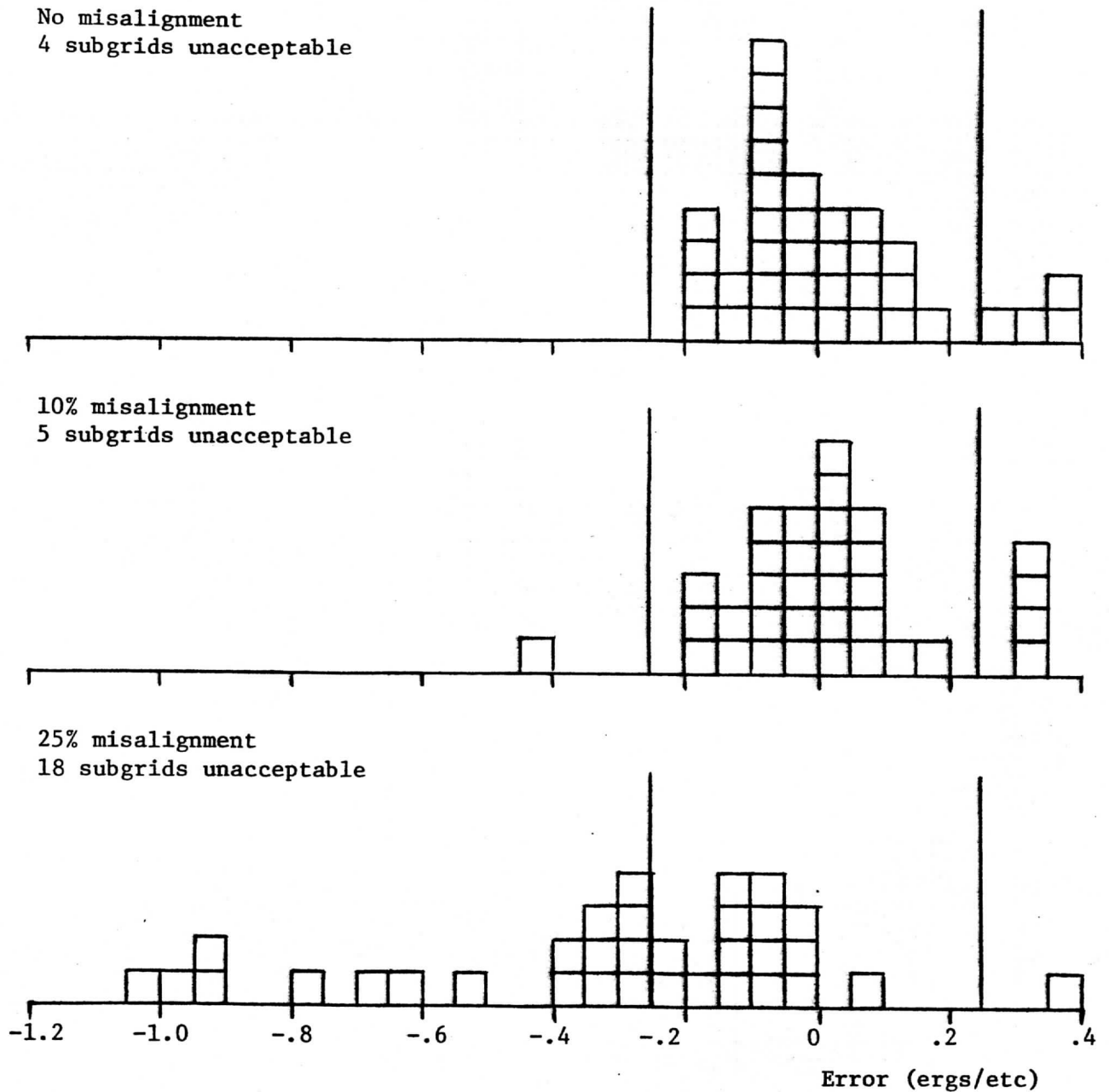of 10 noise runs (average noise RMS per subgrid = .13 erg/etc).

FIGURE 11

Weighted Mean Error with gate = σ for difference misalignments on 60 x 60 Km
CIG subgrids viewed with real detector response; average of 10 noise runs
(average noise RMS per subgrid = .20 erg/etc).

No misalignment
4 subgrids unacceptable

10% misalignment
5 subgrids unacceptable

25% misalignment
18 subgrids unacceptable

-1.2   -1.0   -.8   -.6   -.4   -.2   0   .2   .4

Error (ergs/etc)

FIGURE 12

Weighted Mean Error with gate = σ for different misalignments on
30 x 30 km CIG subgrids viewed with real detector response; average
of 10 noise runs (average noise RMS per subgrid = .36 erg/etc).

No misalignment
37 of 144 subgrids
    unacceptable
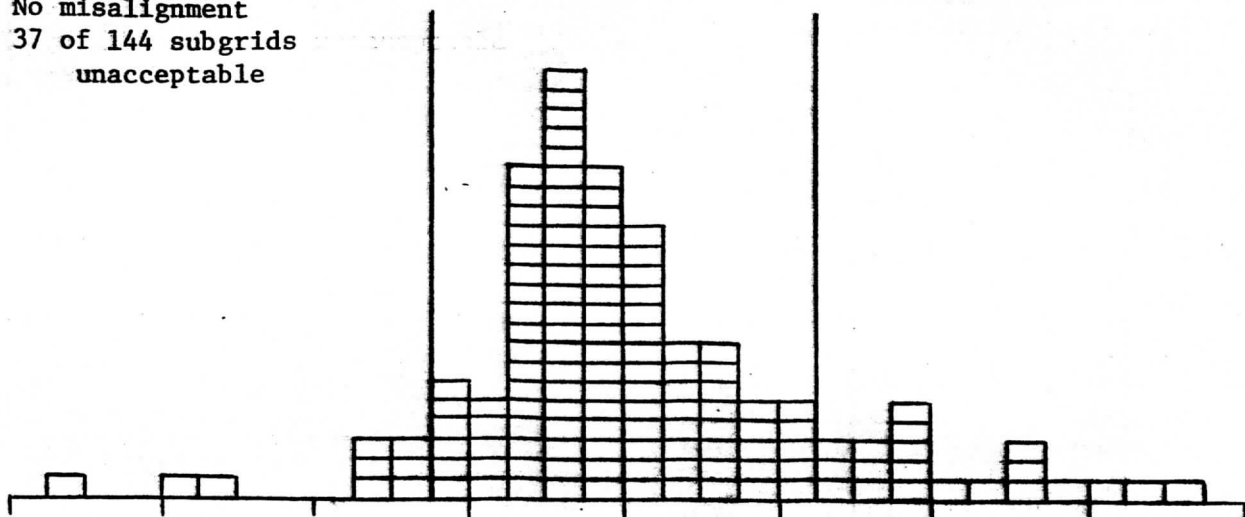
10% misalignment
49 of 144 subgrids unacceptable
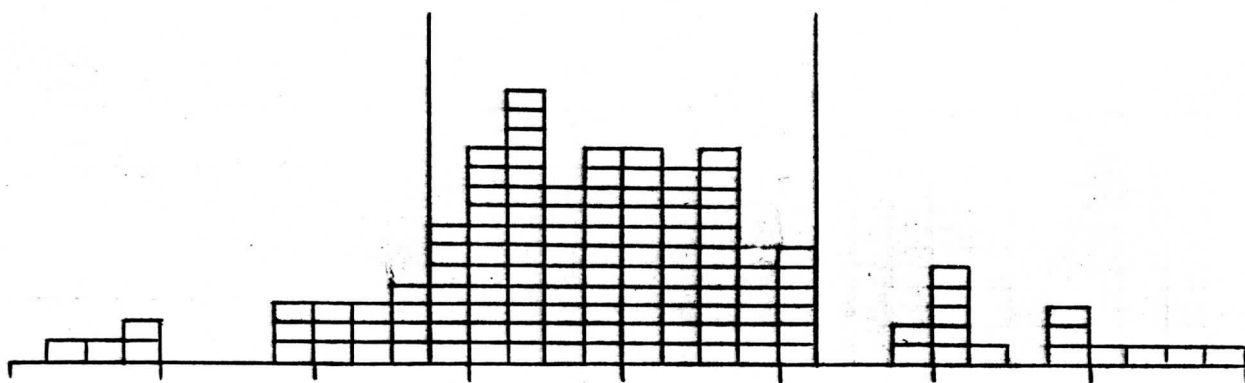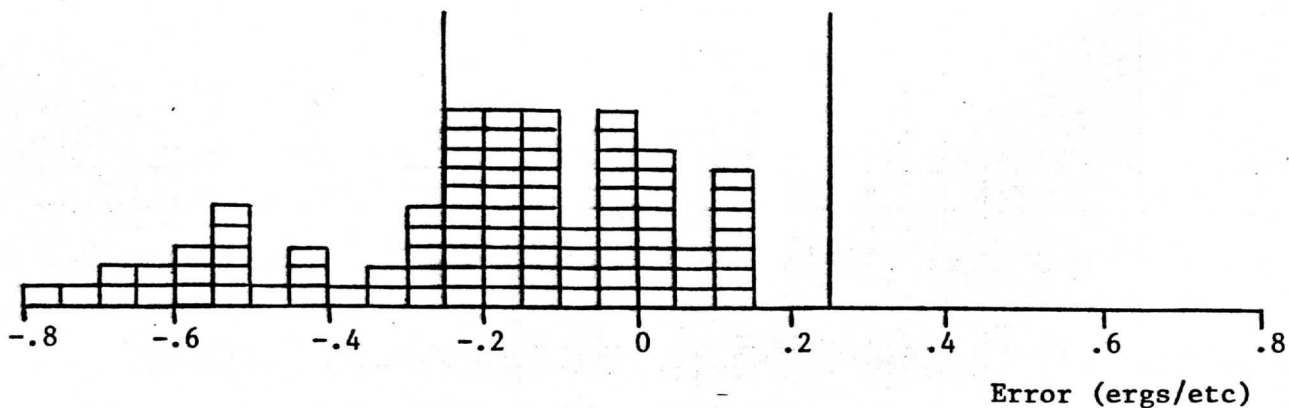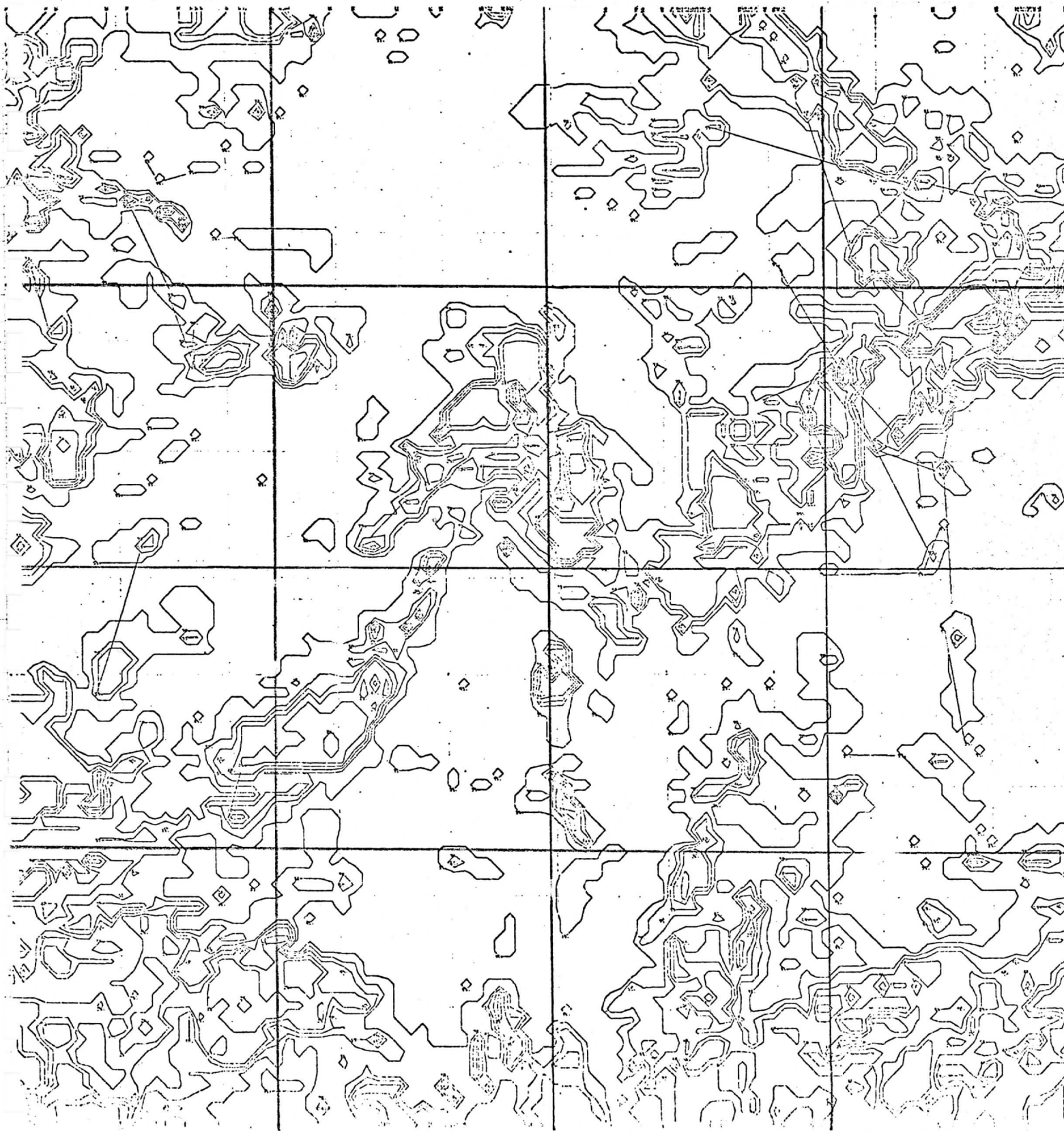
25% misalignment
82 of 144 subgrids unacceptable

-.8   -.6   -.4   -.2   0   .2   .4   .6   .8

Error (ergs/etc)

FIGURE 13

Canary Island Grid   ↑N